Enhancing the charging performance of a triplex-tube thermal energy storage system using fins and nanoparticles

Shahraki, Ali; Tavakoli, Ali; Mohammadi, Majid; Ebrahimi, Amin; Kianifar, Ali

DOI
10.1016/j.tsep.2025.103565

Publication date
2025

Document Version
Final published version

Published in
Thermal Science and Engineering Progress

Citation (APA)
Shahraki, A., Tavakoli, A., Mohammadi, M., Ebrahimi, A., & Kianifar, A. (2025). Enhancing the charging performance of a triplex-tube thermal energy storage system using fins and nanoparticles. *Thermal Science and Engineering Progress*, *62*, Article 103565. https://doi.org/10.1016/j.tsep.2025.103565

Thermal Science and Engineering Progress 62 (2025) 103565

Contents lists available at ScienceDirect

Thermal Science and Engineering Progress

journal homepage: www.sciencedirect.com/journal/thermal-science-and-engineering-progress

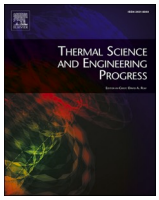

Enhancing the charging performance of a triplex-tube thermal energy storage system using fins and nanoparticles

Ali Shahraki [a], Ali Tavakoli [b], Majid Mohammadi [a], Amin Ebrahimi [c], Ali Kianifar [a,*]

[a] Department of Mechanical Engineering, Engineering Faculty, Ferdowsi University of Mashhad, Mashhad, Iran
[b] Department of Engineering Mechanics, Xi'an Jiaotong University, No. 28, West Xianning Road, Xi'an, Shaanxi 710049, China
[c] Faculty of Mechanical Engineering, Delft University of Technology, Mekelweg 2, 2628CD Delft, The Netherlands

ARTICLE INFO

Keywords:
Triplex tube heat exchanger
Thermal energy storage
Nano enhanced phase change materials
Fin configuration

ABSTRACT

This study explores the enhancement of charging performance in a triplex-tube latent heat thermal energy storage system (TTHX) by integrating longitudinal fins and alumina nanoparticles in phase change materials (PCMs). Numerical simulations are conducted to systematically examine the influence of fin length, thickness, number, and orientation, alongside the impact of nano-enhanced PCMs (NEPCMs) to identify optimal configurations for improved charging performance. The results show that incorporating fins accelerates the melting process, with thinner, more numerous fins providing the greatest enhancement. The optimal configuration, consisting of 64 fins with a reduced thickness of 125 μm, achieved an 86% reduction in charging time compared to the baseline case without fins. While adding nanoparticles to the PCM further improved heat transfer, concentrations exceeding 4% led to a decline in the system's overall thermal storage capacity. Among the PCMs studied, RT80-HC outperformed RT82 due to its higher latent heat of fusion and narrower phase-change temperature range. Additionally, horizontal fin configurations demonstrated a slight advantage by increasing the solid–liquid interface area, further enhancing melting efficiency. This study provides a comprehensive analysis of fin optimization and NEPCM integration in TTHXs, offering a better insight into maximizing thermal energy storage performance. The findings contribute to the development of more efficient latent heat thermal energy storage systems, supporting advancements in renewable energy utilization.

1. Introduction

Solar thermal energy holds great potential as a renewable energy source, however its intermittent nature poses challenges for consistent energy supply [1,2]. To address this issue, thermal energy storage systems, particularly latent heat thermal energy storage systems (LHTESS), are attractive due to their high energy storage capacity and ability to maintain nearly constant temperatures during energy storage and release [3,4]. LHTESS relies on phase change materials (PCMs), which store and release energy through phase transitions, typically between solid and liquid states [5]. However, the widespread adoption of LHTESS is hampered by the inherently low thermal conductivity of most PCMs, which limits the efficiency of charging and discharging processes [5,6].

Organic PCMs are often preferred over inorganic alternatives due to their favorable properties, such as thermal stability, chemical inertness, non-corrosiveness, and cost-effectiveness [7]. They also exhibit high latent heat capacity, consistent melting behavior, minimal phase segregation, and negligible volume changes during phase transitions [6]. These characteristics make organic PCMs suitable for diverse applications, including building energy storage, waste heat recovery, and battery thermal management [8]. Despite these advantages, the low thermal conductivity of PCMs remains a critical limitation that must be addressed to improve the performance of LHTESS.

To enhance the thermal conductivity of PCMs, various strategies such as the use of fins [9] and the dispersion of nanoparticles within PCM [10], have been explored. Fins are widely employed due to their simplicity, cost-effectiveness, and ability to improve heat transfer rates [11,12]. Similarly, the addition of nanoparticles, particularly metal oxides like alumina (Al_2O_3), has been shown to significantly enhance the thermal conductivity of PCMs [2]. Alumina nanoparticles are particularly favored due to their stability, availability, and superior thermophysical properties [13,14]. Among the various configurations of LHTESS, triplex-tube heat exchangers (TTHXs) have gained attention for their ability to facilitate simultaneous charging and discharging, thereby improving overall system efficiency [15,16]. Previous studies have

* Corresponding author.
E-mail addresses: a.ebrahimi@tudelft.nl (A. Ebrahimi), a-kiani@um.ac.ir (A. Kianifar).

https://doi.org/10.1016/j.tsep.2025.103565
Received 4 October 2024; Received in revised form 14 February 2025; Accepted 3 April 2025
Available online 6 April 2025

Nomenclature

b	fins thickness (mm)
C	mushy zone constant $\left(\text{kg m}^{-2}\text{ s}^{-2}\right)$
C_p	specific heat $\left(\text{J kg}^{-1}\text{ K}^{-1}\right)$
d	fins length (mm)
g	gravity acceleration
h	sensible enthalpy $\left(\text{J kg}^{-1}\right)$
H	enthalpy $\left(\text{J kg}^{-1}\right)$
ΔH	latent heat
k	thermal conductivity $\left(\text{W m}^{-1}\text{ K}^{-1}\right)$
L	latent heat of fusion $\left(\text{J kg}^{-1}\right)$
P	pressure (Pa)
T	temperature of PCM (K)
u_i	fluid velocity in the i-direction

Greek letter

β	Thermal expansion coefficient $\left(\text{K}^{-1}\right)$
λ	liquid fraction
μ	Dynamic viscosity $\left(\text{kg m}^{-1}\text{ s}^{-1}\right)$
ρ	Density of PCM $\left(\text{kg m}^{-3}\right)$
φ	volume fraction (concentration)

Subscripts

f	fin
l	liquid state
m	melting range
n	Nanoparticles
ref	At reference temperature
s	solid state
t	total

Abbreviation

HTF	Heat Transfer Fluid
HC	Higher latent heat Capacity
LHTESS	latent heat thermal energy storage systems
NEPCM	nano-enhanced PCM
PCM	phase change material
RT	Rubitherm
TTHX	Triplex-Tube Heat Exchanger

attempted to optimize TTHXs by exploring different fin geometries, sizes, and materials, as well as the impact of nanoparticle-enhanced PCMs [17–21]. For instance, Liu and Tao [22] demonstrated that longitudinal fins outperform annular fins in enhancing LHTESS performance, while Al-Abidi et al. [23,24] highlighted the significant influence of fin parameters (thickness, length, and number) on the charging rate of TTHXs.

Despite these advancements, several research gaps remain. While the benefits of fins and nanoparticles on LHTESS performance are well-documented, the specific effects of varying fin parameters (e.g., number, length, and thickness) on the melting process in TTHXs have not been fully explored. Additionally, there is limited research on the optimal nanoparticle volume fraction for enhancing energy storage in TTHXs. Furthermore, new paraffin materials with higher latent heat of fusion, such as RT80-HC, and the impact of fin orientation (horizontal versus vertical) on system efficiency have not been thoroughly investigated. This study addresses these gaps by systematically examining the effects of fin incorporation and nanoparticle dispersion on the melting process in a triplex-tube thermal energy storage system. The influence of fin number, length, and thickness on system performance is investigated while maintaining a constant PCM volume. The optimal nanoparticle volume fraction for enhancing thermal conductivity is determined, and the performance of RT80-HC paraffin is compared with RT82 paraffin in terms of melting time and total thermal energy storage. Additionally, the impact of fin orientation on system efficiency is evaluated by comparing novel horizontal and vertical configurations with conventional designs. The novelty of this research lies in its comprehensive approach to optimizing fin parameters and nanoparticle dispersion within a TTHX, as well as its exploration of new PCM materials and fin orientations, which, to the best of the authors' knowledge, have not been previously addressed in the literature. This work contributes to the advancement of LHTESS optimization and provides valuable insights for designing more efficient thermal energy storage systems, thereby supporting the broader goal of sustainable energy utilization.

2. Problem statement and formulation

2.1. Physical model

The triplex-tube heat exchanger (TTHX) analyzed in this study consists of three concentric tubes, forming three distinct regions that facilitate efficient thermal energy storage and transfer. The middle region, located between the inner and middle tubes, is filled with phase change material (PCM) and serves as the thermal energy storage medium. The inner and outer regions contain the heat transfer fluid (HTF) that transfers thermal energy to and from the PCM. The dimensions of the TTHX are based on the work of Al-Abidi et al. [24]. The inner, middle, and outer tubes have diameters of 50.8 mm, 150 mm, and 200 mm, respectively, with corresponding thicknesses of 1.2 mm, 2 mm, and 2 mm. The total length of the heat exchanger is 500 mm, and the system is oriented horizontally. Water is used as the HTF due to its cost-effectiveness and favorable thermophysical properties. In cases where nano-enhanced PCMs (NEPCMs) are considered, alumina nanoparticles are uniformly dispersed within the PCM to improve thermal conductivity. The TTHX and fins are made of copper, selected for its high thermal conductivity. The thermophysical properties of the materials used in this study, including PCMs, nanoparticles, and TTHX materials, are assumed to be constant and temperature-independent [25]. These

Table 1
Thermophysical properties of the materials used in the study, including PCMs, nanoparticles, and TTHX components. Data is taken from [24,26].

Property	PCM (RT82)	PCM (RT80-HC)	Alumina (Al_2O_3)	Copper (Cu)
Density in solid state, $\rho_s\left[\text{kg m}^{-3}\right]$	950	900	3600	8978
Density in liquid state, $\rho_l\left[\text{kg m}^{-3}\right]$	770	800	–	–
Specific heat, Cp_s, $Cp_l\left[\text{J kg}^{-1}\text{ K}^{-1}\right]$	2000	2000	0.765	381
Melting temperature range, T_m[°C]	77–85	77–80	–	–
Latent heat of fusion, $L\left[\text{kJ kg}^{-1}\right]$	176	220,000	–	–
Thermal conductivity, $k\left[\text{W m}^{-1}\text{ K}^{-1}\right]$	0.2	0.2	36	387.6
Dynamic viscosity, $\mu\left[\text{kg m}^{-1}\text{ s}^{-1}\right]$	0.03499	0.03499	–	–
Thermal expansion coefficient, $\beta\left[\text{K}^{-1}\right]$	0.001	0.001	–	–

properties are summarized in Table 1. This study systematically investigates the effects of various fin configurations, including fin length, thickness, number, and orientation, along with the impact of nanoparticle dispersion and different PCM materials on the thermal performance of the TTHX. The specific parameters and variations examined are detailed in Table 2.

2.2. Mathematical model

To model the melting process of the PCM in TTHX, several simplifying assumptions were made. The PCM flow was considered incompressible, transient, and laminar, with negligible viscous dissipation effects. The influence of natural convection was accounted for using the Boussinesq approximation in the energy equation, which incorporates buoyancy forces due to density variations. The thermophysical properties of the PCM were assumed to be constant, and heat transfer between the TTHX and its surroundings was neglected. Additionally, volume changes in the PCM during phase transition were not considered. Accordingly, the governing equations for mass, momentum, and energy conservation in the PCM region were formulated, respectively, as shown in Eq. (1) to (3) [27]:

$$\partial_i(\rho u_i) = 0 \tag{1}$$

$$\partial_t(\rho u_i) + \partial_i\left(\rho u_i u_j\right) = \mu\partial_{jj}u_i - \partial_i p + \rho g_i + S_i \tag{2}$$

$$\partial_t(\rho h) + \partial_t(\rho\Delta H) + \partial_i(\rho u_i h) = \partial_i(k\partial_i T) \tag{3}$$

where u_i is the fluid velocity in the i-direction, ρ is the density of PCM, μ is the dynamic viscosity, p is the pressure, g is the gravity acceleration, h is the sensible heat, ΔH is the latent heat and k is the thermal conductivity of PCM.

The sensible heat of the PCM was defined as a function of temperature, while the total enthalpy was expressed as the sum of sensible and latent heat components. Eq. (4) determines the total enthalpy of PCM defined as [28]:

$$H = h + \Delta H \tag{4}$$

Table 2
Summary of studied cases, detailing variations in fin length, thickness, number, orientation, nanoparticle dispersion, and PCM selection in the TTHX.

Model	Case #	Number of fins	φ_f	φ_n	b [mm]	d [mm]
Fin length	1	0	0.0	–	1	0
	2	8	0.005	–	1	10
	3	8	0.01	–	1	20
	4	8	0.015	–	1	30
	5	8	0.02	–	1	40
	6	8	0.024	–	1	48.4
Fin thickness	7	8	0.04	–	2	40
	8	8	0.06	–	3	40
	9	8	0.08	–	4	40
Fin numbers	10	4	0.01	–	1	40
	11	6	0.015	–	1	40
Nanoparticles concentration	12	0	–	0.02	–	–
	13	0	–	0.04	–	–
	14	0	–	0.08	–	–
PCMs (PCM RT80-HC)	15	8	0.02	–	–	40
Fin contact angle						
Horizontal fins	16	8	0.02	–	1	40
Vertical fins	17	8	0.02	–	1	40
Fin thickness and number	18	16	0.02	–	0.5	40
	19	32	0.02	–	0.25	40
	20	64	0.02	–	0.125	40
Fin length and number	21	12	0.02	–	1	26.6
	22	16	0.02	–	1	20
	23	20	0.02	–	1	16.8
	24	32	0.02	–	1	10

where, the sensible heat (h) can be expressed as Eq. (5) [29]:

$$h = h_{ref} + \int_{T_{ref}}^{T} c_p dT. \tag{5}$$

The latent heat can be expressed by Eq. (6) [30,31]:

$$\Delta H = \lambda \cdot L \tag{6}$$

where h_{ref} is reference enthalpy at reference temperature (T_{ref}), c_p is the specific heat capacity of PCM at constant pressure L is the latent heat of fusion and λ is the liquid fraction of PCM that ranges between 0 (for solid) to 1 (for liquid) and can be computed by Eq. (7) [12,32]:

$$\lambda = \begin{pmatrix} 0 & \text{if} & T < T_s \\ 1 & \text{if} & T > T_l \\ \dfrac{T - T_s}{T_l - T_s} & \text{if} & T_l > T > T_s \end{pmatrix} \tag{7}$$

Eqs. (8) and (9) showed how to calculate the density of PCM [30]:

$$\rho = \rho_m \cdot (1 - \beta \cdot (T - T_m)) \tag{8}$$

$$T_m = \frac{T_l + T_s}{2}. \tag{9}$$

where, ρ_m is the density of PCM in the liquid phase, β is the thermal expansion coefficient and T_m is the average temperature of PCM [33].

The enthalpy-porosity technique [27] was used to model solidification and melting in the simulations. Hence, the following source term (Eq. (10) was added to the momentum equation to suppress fluid velocities in solid regions [34]:

$$S_i = C \cdot (1 - \lambda)^2 \cdot \frac{u_i}{\lambda^3 + \varepsilon} \tag{10}$$

here, C is the mushy-zone constant, which is 10^5 based on the criterion defined by Ebrahimi et al. [35]. ε is a small constant (10^{-3}) to avoid division by zero.

For nano-enhanced PCMs (NEPCMs), the effective density, specific heat capacity, and latent heat were calculated using equilibrium mixture models. The dynamic viscosity and thermal conductivity were estimated based on established correlations 11 to 13 that incorporate the effects of nanoparticle Brownian motion. Accordingly, the effective density, specific heat capacity and latent heat were approximated using the following expressions, respectively [36,37]:

$$\rho_{npcm} = \varphi_n \cdot \rho_{np} + (1 - \varphi_n) \cdot \rho_{pcm} \tag{11}$$

$$\left(\rho \cdot c_p\right)_{npcm} = \varphi_n \cdot \left(\rho \cdot c_p\right)_{np} + (1 - \varphi_n) \cdot \left(\rho \cdot c_p\right)_{pcm} \tag{12}$$

$$\left(\rho \cdot L_f\right)_{npcm} = (1 - \varphi_n) \cdot \left(\rho \cdot L_f\right)_{pcm} \tag{13}$$

The dynamic viscosity and thermal conductivity of the NEPCMs were modeled using expressions developed by Vajjha et al. [36], incorporating the effects of Brownian motion of nanoparticles. φ_s is the percentage of occupied volume by solids (fins or nanoparticles) [25] and can resulted in:

$$\varphi_s = \frac{V_s}{V_t} \tag{14}$$

In the simulations, the heat transfer fluid (HTF) was maintained at a constant inlet temperature of 90°C throughout the melting process, while the PCM was initially set at 27°C in its solid state. The use of a constant HTF temperature as a boundary condition has been validated by showing good agreement with empirical model results [25]. The boundary conditions applied were as follows: at the inner radius ($r = R_1$) and outer radius ($r = R_2$) of the PCM region, the temperature was fixed at 90°C. Additionally, at the initial time ($t = t_0$), the temperature of the HTF

was set to 90°C. The applied boundary conditions were consistent with those used in previous studies [24], ensuring reliable comparisons with experimental data.

2.3. Numerical implementation

The phase change process in the triplex-tube heat exchanger (TTHX) was simulated using ANSYS Fluent 16.0, a computational fluid dynamics (CFD) software based on the finite-volume method. A pressure-based solver with double precision was employed to ensure numerical accuracy. The Quadratic Upstream Interpolation for Convective Kinematics (QUICK) scheme was used to discretize the governing equations, while the Semi-Implicit Method for Pressure-Linked Equations (SIMPLE) algorithm was applied to couple the pressure and velocity fields. The Pressure Staggered Option (PRESTO) scheme was selected for pressure interpolation, and second-order upwind schemes were used for the momentum and energy equations. To maintain numerical stability, under-relaxation factors were set to 0.3 for pressure, 0.4 for velocity, 1.0 for energy, and 0.4 for the liquid fraction. Convergence criteria required scaled residuals to reach 10^{-3} for continuity and momentum equations and 10^{-6} for the energy equation at each time step. To optimize computational resources, a half-section model of the TTHX was used for most simulations, except in cases involving six fins, where the full geometry was necessary to accurately capture flow dynamics (Fig. 1).

3. Model verification

3.1. Grid independence and time step independence analysis

To ensure the accuracy and efficiency of the numerical model, a grid independence and time step independence analysis was conducted for Case 6, and the results are presented in Fig. 2. (a) Three different grid resolutions (with 13,718, 17,006, and 22,000 cells) were examined to determine the optimal grid size. The liquid fraction during the melting process was analyzed for each grid size. The difference in liquid fraction between the 17,006 and 22,000 grid cases was minimal, at just 0.52%, indicating that further refinement beyond 17,006 grids offers negligible improvements. In contrast, the difference between the 13,718 and 17,006 grid cases was more pronounced at 4%. To balance computational efficiency with accuracy, the grid size of 17,006 was selected for subsequent simulations.

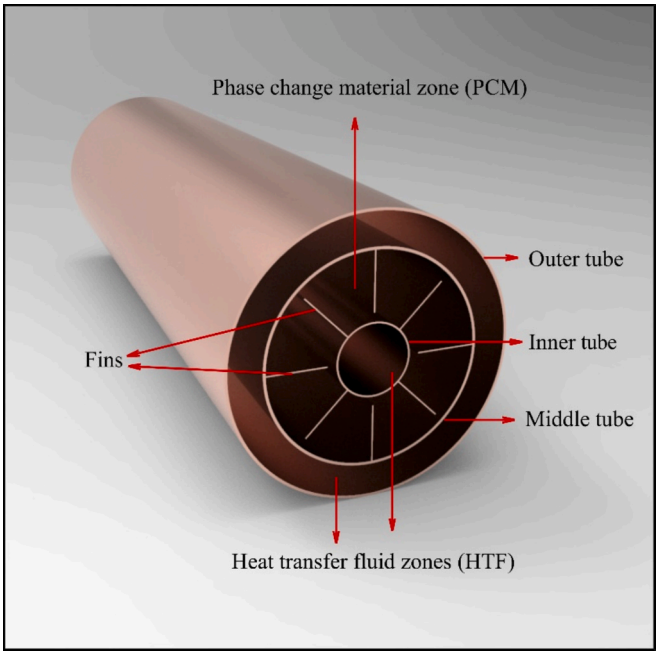

Fig. 1. Schematic of the triplex-tube heat exchanger (TTHX) with eight longitudinal fins.

The impact of different time steps (0.01, 0.05, 0.1, and 0.5 s) on the results was also evaluated for Case 6. The analysis showed that the difference in liquid fraction values predicted using time steps of 0.05 and 0.1 s was only 0.005%, which is negligible. Therefore, a time step of 0.1 s was chosen. This choice ensures that the model is both accurate and computationally efficient. The results of the grid size and time step independence analyses are illustrated in Fig. 2, which shows the variation in liquid fraction during the PCM melting process under the different conditions tested.

3.2. Model validation

The numerical model developed for the TTHX was validated against both experimental and numerical results reported by Al-Abidi et al. [24]. The same boundary conditions, initial conditions, and material properties were used to ensure a consistent comparison. Fig. 3 shows the present numerical predictions in comparison to the data reported by Al-Abidi et al. [38]. During the initial phase of the simulation, up to 500 s, the temperatures obtained from the model showed some discrepancies compared to the experimental data. This deviation was primarily observed in the regions near the tube walls, where temperature rise was more pronounced in the numerical predictions. In Al-Abidi's experiments, thermocouples were not in direct contact with the tube walls, which explains the absence of this initial temperature rise in their experimental results. Consequently, the higher average temperature observed in the numerical simulation is considered reasonable. After the initial 500 s, the numerical results aligned more closely with both Al-Abidi's experimental and numerical data, as shown in Fig. 3 The higher average temperatures predicted by the numerical model are reasonable given the absence of environmental heat losses in the simulations. This validation confirms that the model accurately represents the thermal behavior of the TTHX system, particularly after the initial phase of the melting process.

4. Results and discussion

4.1. The influence of conjugated heat transfer

At the start of the melting process in the triplex-tube heat exchanger (TTHX), heat transfer within the phase change material (PCM) is primarily governed by thermal conduction [39]. This is due to the limited amount of molten PCM, which restricts the effects of natural convection. As the melting process progresses and more liquid PCM forms, natural convection becomes increasingly dominant, significantly enhancing heat transfer. However, in the lower regions of the TTHX, where molten material movement is minimal, conduction remains the primary heat transfer mechanism. To improve heat transfer in these conduction-dominated regions, the use of extended surfaces, such as fins, is particularly effective. Fins enhance heat transfer by increasing the contact area between the PCM and the heat exchanger walls. A symmetrical fin arrangement is preferred to ensure balanced thermal performance during both the charging (melting) and discharging (solidification) phases of the thermal cycle [40,41].

The numerical simulations show the critical role of solid components, including the TTHX walls and fins, in influencing the heat transfer process. The results shown in Fig. 4 demonstrate that when conjugate heat transfer is considered in the model, a reduction in PCM melting time is observed compared to simulations that neglect heat transfer through solid regions. Specifically, neglecting heat conduction in the solid components results in an 11.39% underestimation of the melting time. This underscores the importance of accurately modeling heat conduction within the TTHX structure to obtain realistic predictions of system performance.

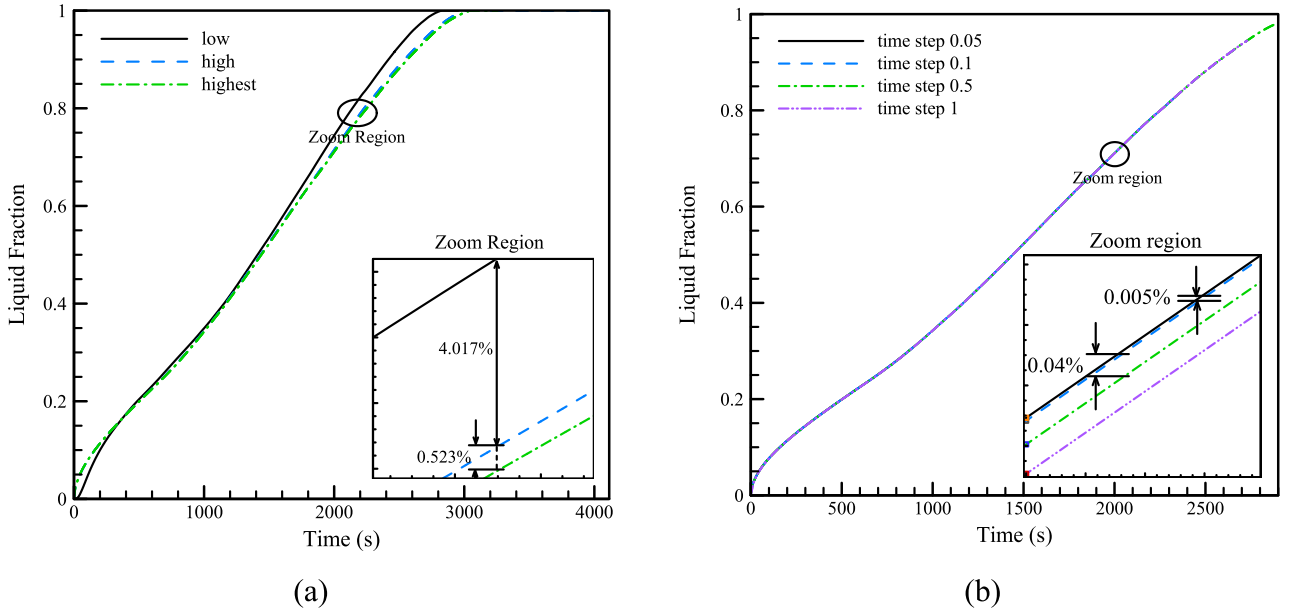

Fig. 2. (a) Effect of grid size on the predicted liquid fraction. (b) Influence of time-step size on the numerical simulation results.

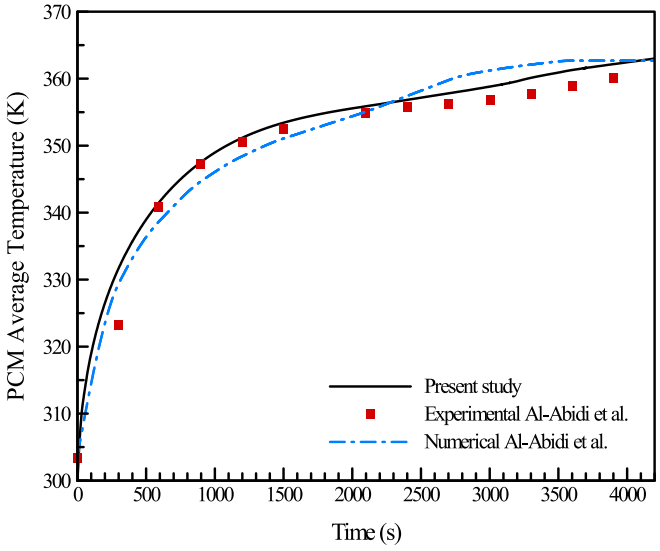

Fig. 3. Validation of the present numerical model against experimental and numerical data from Al-Abidi et al. [14].

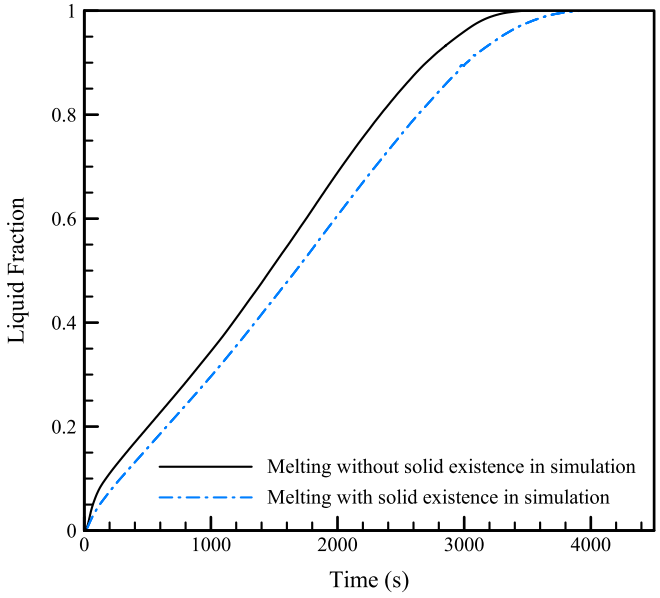

Fig. 4. Influence of conjugate heat transfer on the PCM melting process, highlighting the effect of solid components in the TTHX.

4.2. Cases with variable PCM volume in the system

4.2.1. The effect of fin length

The impact of fin length on the charging performance of the TTHX was analyzed by varying the fin length while keeping the number of fins constant at eight. The tested fin lengths were 10 mm, 20 mm, 30 mm, 42 mm, and 48.4 mm. Longer fins increase the surface area for heat transfer, improving energy distribution within the PCM and accelerating the melting process.

The results in Fig. 5 indicate that increasing the fin length significantly reduces the charging time, but with diminishing returns at greater lengths. For instance, the charging time for the system with 42 mm fins was 6.28% shorter than that of the 30 mm fin configuration. Extending the fins to 48.4 mm further reduced the melting time by 9.61% compared to the 42 mm case. However, longer fins also increase system weight and manufacturing complexity, which must be considered in practical applications.

The results presented in Fig. 6 show that the melting times for the tested fin lengths were 6990 s (10 mm), 5540 s (20 mm), 4480 s (30 mm), 3950 s (42 mm), and 3000 s (48.4 mm). Corresponding heat flux values were 245.8 W/m^2, 306.8 W/m^2, 377.5 W/m^2, 423.3 W/m^2, and 460.5 W/m^2, respectively. These findings confirm that increasing fin length enhances heat transfer and reduces melting time, but practical trade-offs related to weight, complexity, and structural integrity must be considered when optimizing fin design.

4.2.2. The effect of fin thickness

Fig. 7 shows the effect of fin thickness on the charging time in a TTHX equipped with eight fins. While increasing the thickness of the fins leads to a reduction in the charging, the impact is insignificant when compared with the effect of fin length. Specifically, the total melting times for Cases 5, 7, 8, and 9, corresponding to fin thicknesses of 1 mm,

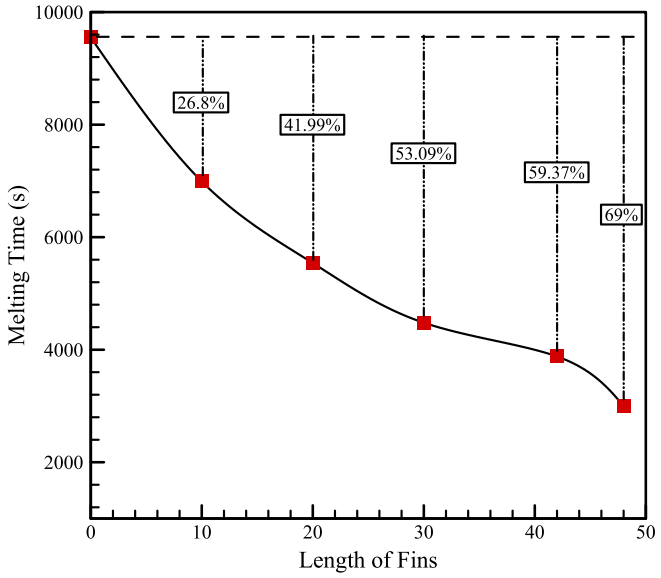

Fig. 5. Effect of fin length on melting time, showing the relationship between fin extension and heat transfer efficiency.

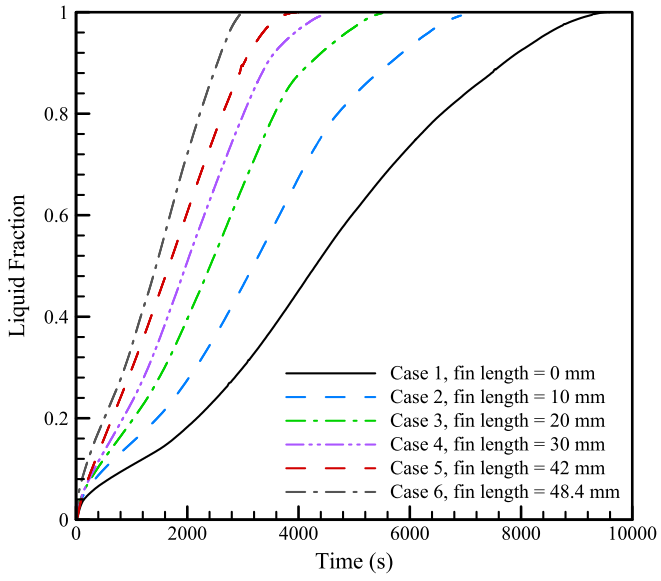

Fig. 6. Influence of fin length on melting time in the TTHX.

2 mm, 3 mm, and 4 mm, are 3950 s, 3680 s, 3450 s, and 3130 s, respectively. These results represent improvements in melting time of 6.8%, 12.6%, and 20.7% for the thicker fins when compared to Case 5. However, despite these gains, the overall enhancement achieved by increasing fin thickness is insubstantial. This suggests that while thicker fins can contribute to faster charging, their impact is relatively limited compared to other factors, such as fin length, in optimizing the melting process in the TTHX system.

4.2.3. The effect of fin numbers

The impact of changing the number of fins in a TTHX was studied by increasing the number of fins from 0 to 8 while keeping their length and thickness constant. The results, shown in Fig. 8(a), indicate that increasing the number of fins leads to a reduction in the charging time. Specifically, the melting times for configurations with 0, 4, 6, and 8 fins are 9500 s, 5900 s, 4800 s, and 3950 s, respectively. However, as the number of fins increases, the rate of improvement in melting

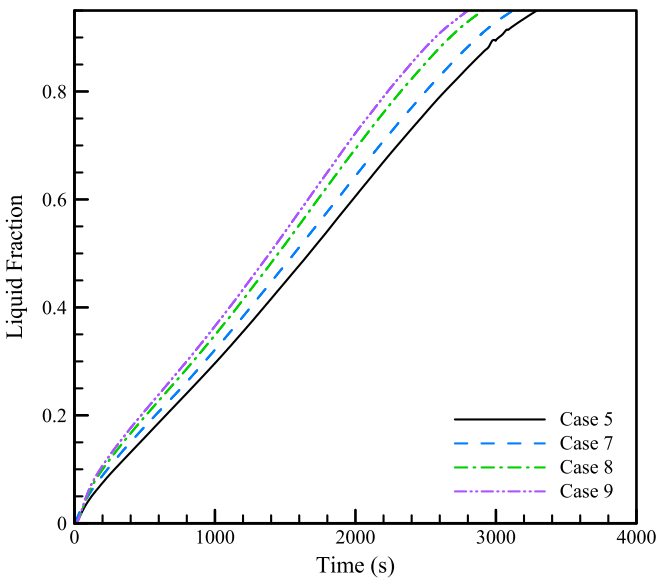

Fig. 7. Effect of fin thickness on the melting fraction, demonstrating the limited impact of thickness variations.

performance decreases. For instance, the improvements in charging time for cases with 4, 6, and 8 fins are 38.21%, 49.73%, and 59.37%, respectively, compared to the case with no fins.

Fig. 8(b) demonstrates that adding more fins reduces the volume of PCM available, which in turn decreases the overall energy storage capacity of the TTHX system. The energy stored in cases with 4, 6, and 8 fins is 1.752 MJ, 1.675 MJ, and 1.672 MJ, respectively. Despite this reduction in energy storage capacity, the increase in the number of fins enhances the heat flux from the heat transfer fluid to the PCM, making the addition of fins a logical choice to improve the system's charging performance. The findings suggest that a design with fewer and longer fins is more effective at reducing charging time than one with a greater number of shorter fins for a system with a fixed PCM volume. This finding indicates that optimizing fin length might be more beneficial than increasing the number of fins for improving the overall efficiency of the thermal energy storage system.

4.2.4. The effect of dispersing nanoparticles in the PCM

Fig. 9 shows the effect of incorporating different concentrations (2%, 4%, and 8%) of alumina (Al_2O_3) nanoparticles on the performance of NEPCMs in the thermal energy storage system. Alumina nanoparticles were selected for this investigation due to their frequent use compared to other nanomaterials. In Fig. 9(a), two distinct melting fronts (solid–liquid interface) are visible in the TTHX, positioned near the inner and middle tubes. The melting front above the inner tube and below the middle tube shows a higher growth rate, primarily due to the dominance of natural convection. This leads to the formation of significant dead zones in the lower right and lower left regions of the TTHX, resulting in an increased charging time.

The addition of nanoparticles to the PCM reduces the total charging time. However, increasing the nanoparticle concentration beyond 4% leads to a noticeable decline in the system's overall energy storage capacity, as depicted in Fig. 9(b). The heat flux values recorded for the NEPCM cases are 196 W m^{-2} for the 2% nanoparticle case (Case 12), 229 W m^{-2} for the 4% case (Case 13), and 241 W m^{-2} for the 8% case (Case 14), with corresponding total energy storage values of 1.78 MJ, 1.917 MJ, and 1.65 MJ, respectively. Case 13, which contains 4% nanoparticles, demonstrates a 10% improvement in charging time compared to the baseline case with pure PCM (Case 1). However, while higher concentrations of nanoparticles in the PCM enhance heat flux and reduce charging time, they also lead to a decrease in total energy

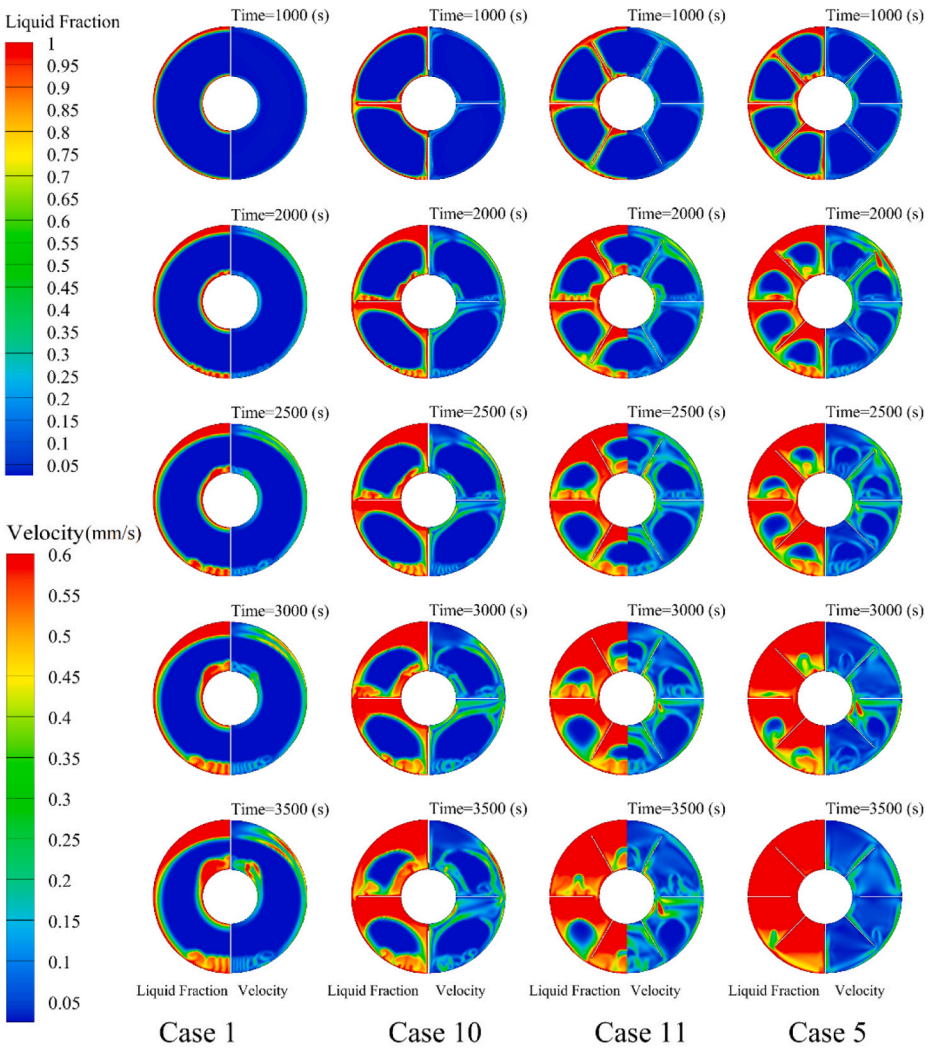

(a)

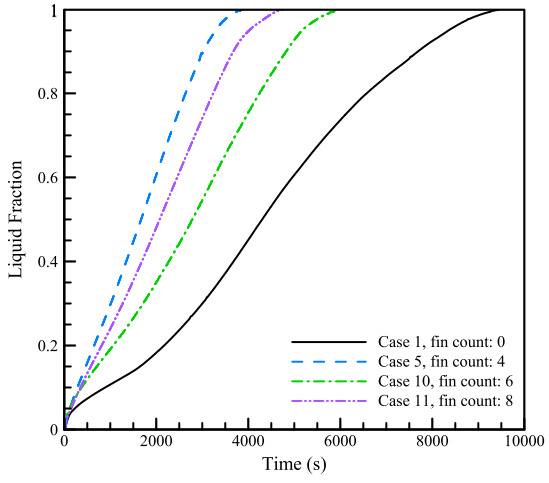

(b)

Fig. 8. (a) Contours of liquid fraction (left) and velocity magnitude (right) during the melting process for different fin numbers. (b) Liquid fraction variation with increasing fin count.

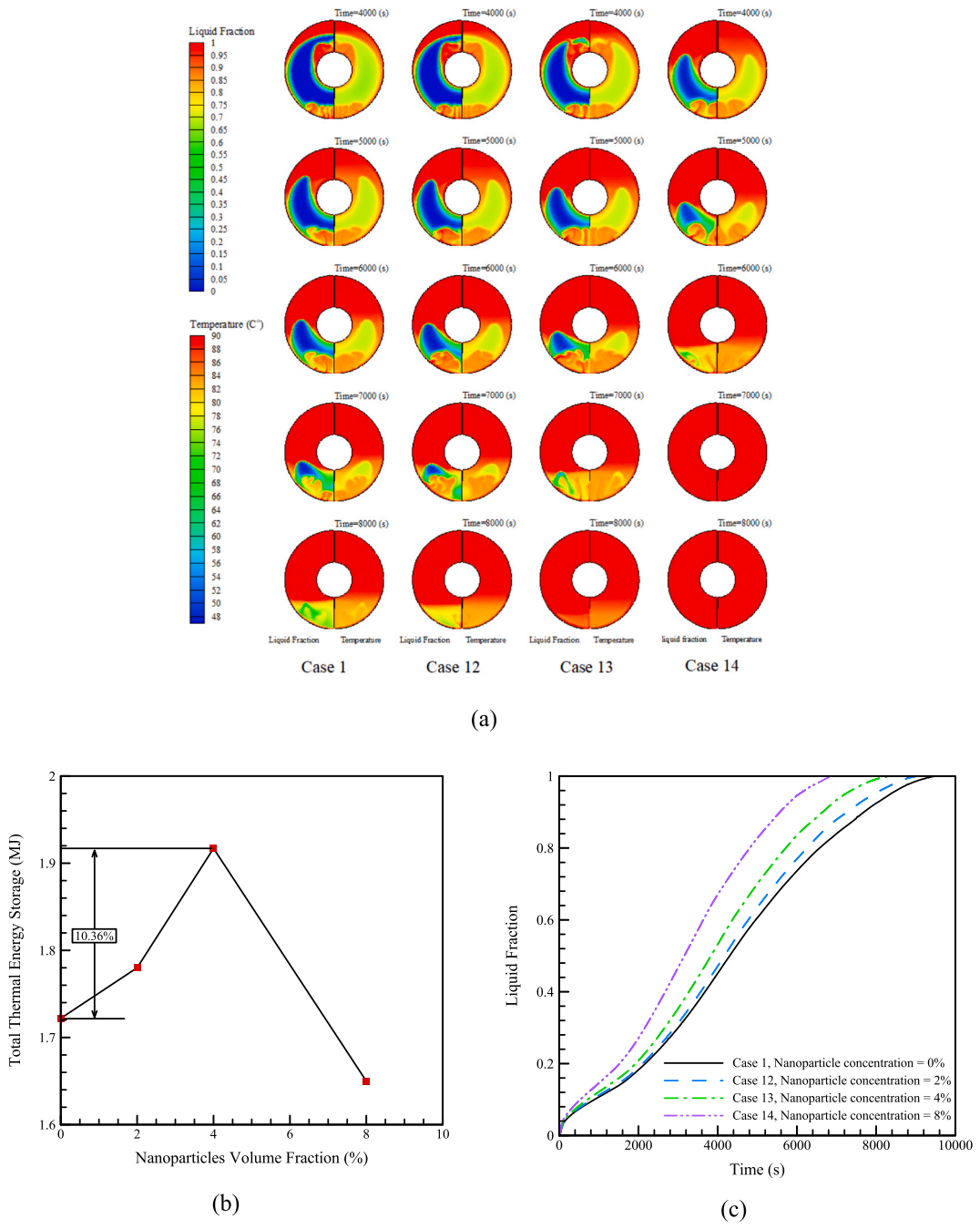

Fig. 9. (a) Liquid fraction (left) and temperature distribution (right) for different NEPCM concentrations. (b) Effect of nanoparticle concentration on total thermal energy storage. (c) Liquid fraction evolution during the melting process for various NEPCM cases.

storage. The data indicates that incorporating more than 4% nanoparticles into the PCM does not provide additional benefits and may even adversely influence the charging time. Furthermore, when comparing the effects of nanoparticles with those of fins, the influence of nanoparticles on charging time is relatively limited. In Cases 12–14, the melting time is improved by 4.9%, 12.3%, and 28.27%, respectively, relative to Case 1. The 4.9% enhancement achieved with 2% NEPCM (Case 12) is minimal compared to the substantial improvements gained by adding fins, making the benefits of nanoparticle incorporation in phase transition systems somewhat insignificant. Nonetheless, in cases where attaching fins is impractical, dispersing nanoparticles in the PCM offers a viable alternative. Fig. 9(c) depicts the melting fraction of all NEPCM cases throughout the melting process. At the first 2000 s of melting process due to conduction domination and temperature difference reduction near of hot walls melting rate decrease through the time. Nanoparticles addition helps in both conduction and convection heat transfer, but limitation of total energy storage is the main challenge in usage of nanoparticles.

4.3. Cases with a fixed PCM volume in the system

4.3.1. The effect of fin contact angle

Fig. 10 illustrates the temperature and liquid fraction distribution contours for three different cases involving horizontal (Case 16), normal (Case 5), and vertical (Case 17) fin configurations. These models implement right-left symmetry in the arrangement of fins. There is a noticeable observation from Fig. 10 that, unlike variations in other parameters of fins, changes in fin angles do not lead to desirable alterations

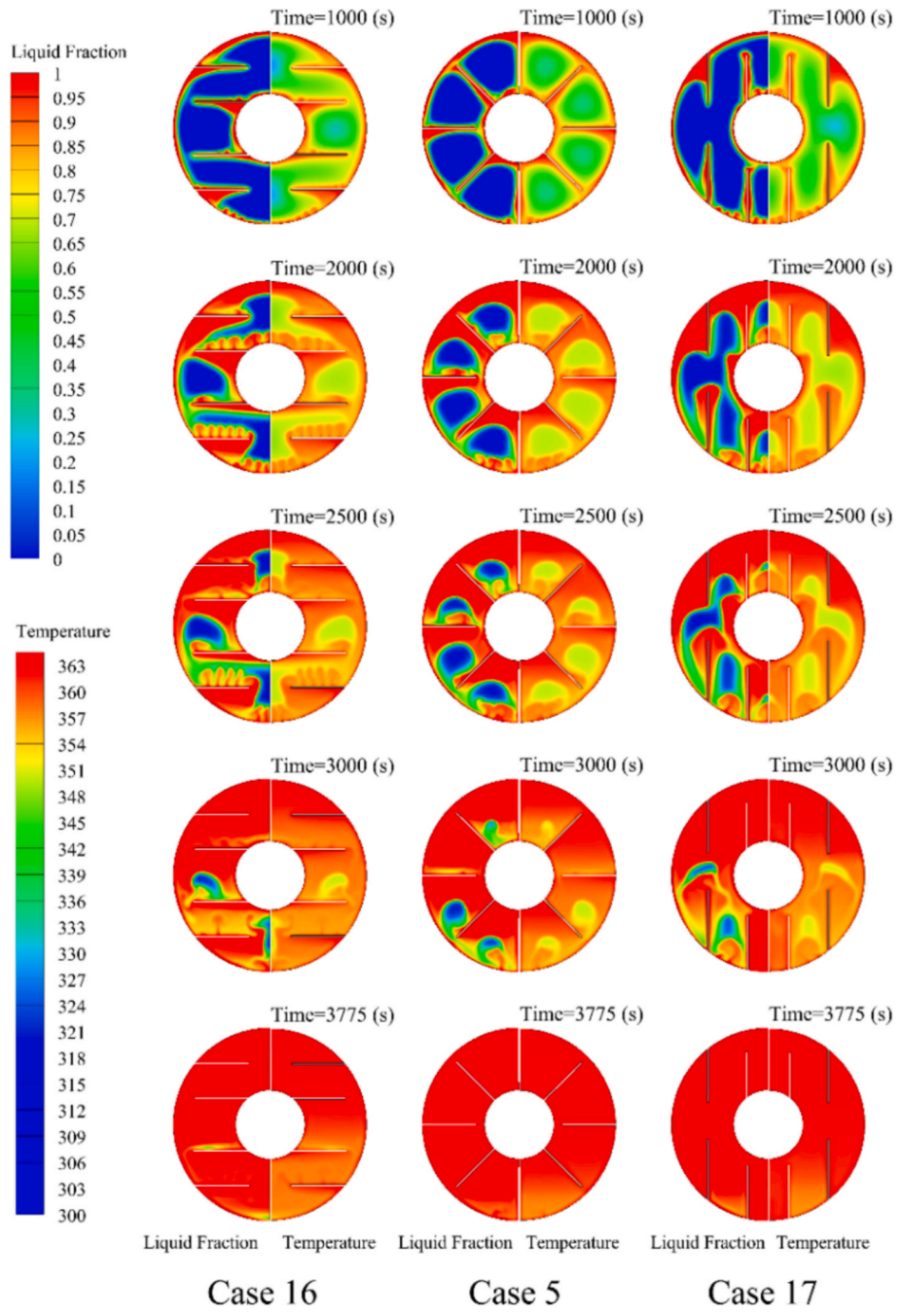

Fig. 10. Liquid fraction (left) and temperature distribution (right) for horizontal, conventional, and vertical fin orientations.

in the melting process. In the vertical fin configuration, the liquid PCM exhibits higher values during the melting process. However, towards the end of the process, all the hot PCM liquids accumulate in the upper half of the thermal energy storage system. This accumulation makes the melting of dead zones more challenging and consequently increases the melting time of Case 17. The melting times for Cases 16, 17, and 5 are 3825 s, 3950 s, and 3950 s, respectively, without any significant difference compared to case 5. It is possible that optimizing the angle of fins may slightly increase the melting rate. Furthermore, Case 16 demonstrates a better enhancement in melting time (3.16% improvement) due to the horizontal configuration of fins, which provides a greater area of unstable liquid–solid interface, resulting in a decrease in melting time [42]. Ultimately, the results indicate that using horizontal fins is more advantageous than employing the conventional fin configuration.

4.3.2. The effect of variations in the fin thickness and number

Fig. 11 illustrates the combined effects of increasing the number of fins and decreasing their thickness on the melting time. Four cases (Cases 5, 18, 19, and 20) are considered, with a varying number of fins: 8 (b = 1 mm), 16 (b = 0.5 mm), 32 (b = 0.25 mm), and 64 (b = 0.125 mm), respectively. All cases maintain a constant fins volume fraction of 2% throughout the changes in fin numbers. It's worth noting that fins with smaller thickness are sometimes referred to as foils, which can be utilized for enhancing heat transfer in (PCMs) [43].

As it can be seen in Fig. 11(a), these cases have a significant impact on the melting time. Compared to Case 1 (no fins), the complete melting time is enhanced by 59.37%, 73.29%, 82.93%, and 86.38% for Cases 5, 18, 19, and 20, respectively, as reported in Fig. 12c. Interestingly, Cases 18 (2550 s), 19 (1630 s), and 20 (1300 s) exhibit significant reductions in melting time. Fortunately, due to the constant volume of PCM in each

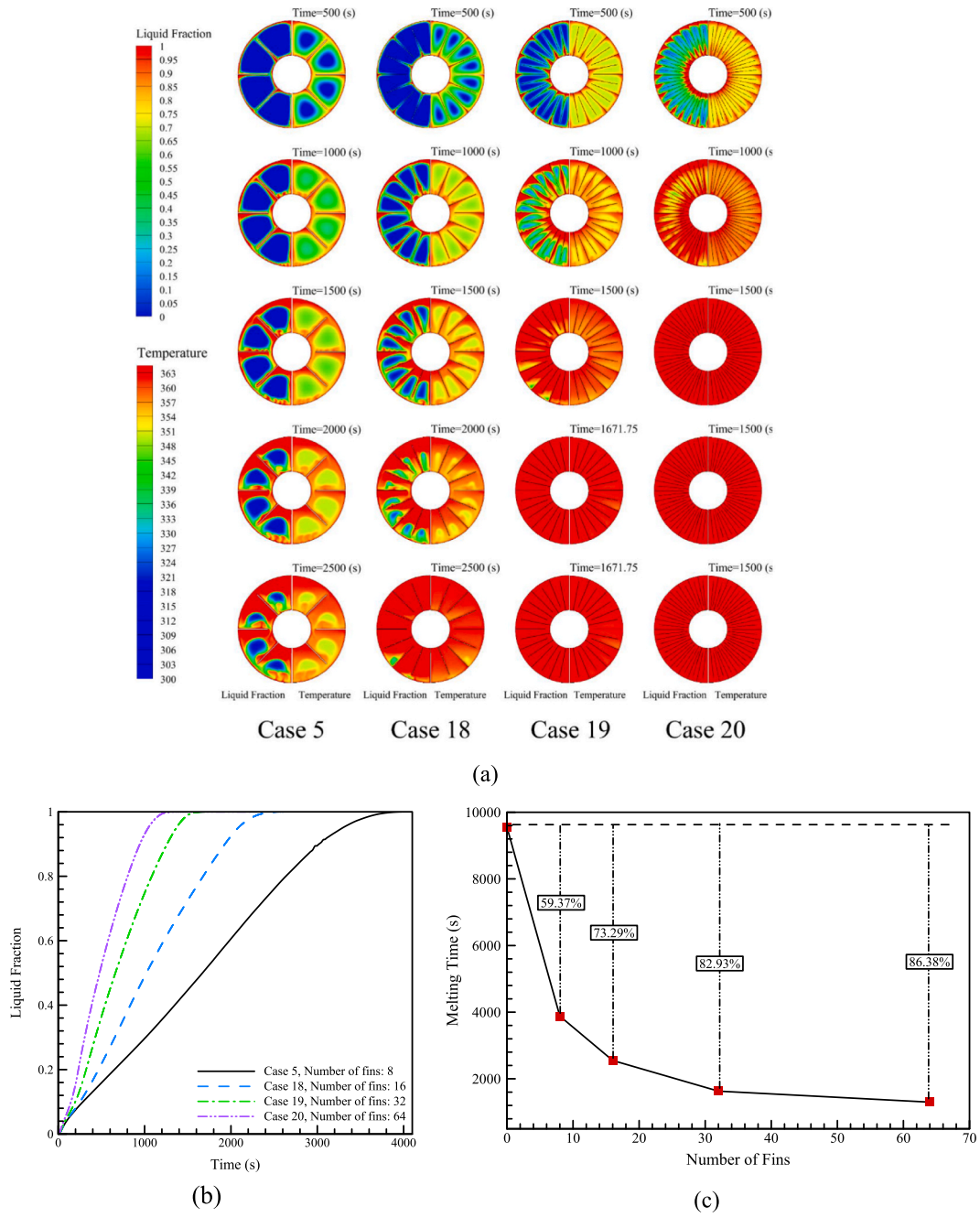

Fig. 11. (a) Liquid fraction (left) and temperature (right) distributions for different fin numbers. (b) The influence of fin thickness-number on the liquid fraction evolution over time. (c) Comparison of the charging time for different fin numbers.

case, the energy storage remains nearly the same.

Varying the thickness and number of fins offers several advantages. One key benefit is a significant increase in the melting rate compared to other designs. Moreover, the volume of the phase change material (PCM) remains the same, ensuring consistent energy storage. However, this approach comes with some challenges. Thinner fins can become fragile and may break during manufacturing or use. Another issue involves how the fins are connected to the tubes. Additionally, enhancing the efficiency of the phase change process requires enlarging the welding area, which can introduce further complications. These challenges pose practical limitations on the utilization of thin and ultra-thin fins. Nevertheless, this model has a profound effect on the PCM melting rate. The increase in the number of fins extends the contact area between PCM and the thermal energy storage system, thereby enhancing heat transfer through conduction. It is important to note that the improvement in complete melting time diminishes as more fins are added. Fig. 11(b) and (c) demonstrates that the addition of 32 fins in Case 19 to Case 20 results in a decrease of 3.4% in melting time compared to Case 1.

4.3.3. *The effect of variations in the fin length and number*

The combined influence of fin length and the number of fins on the thermal performance of the triplex-tube heat exchanger (TTHX) was examined to determine the optimal configuration for enhancing heat transfer while maintaining energy storage capacity. Unlike previous analyses that investigated fin length and number independently, this section explores their combined effect, providing a more comprehensive understanding of their role in optimizing the melting process. In this analysis, multiple fin configurations were studied, with variations in

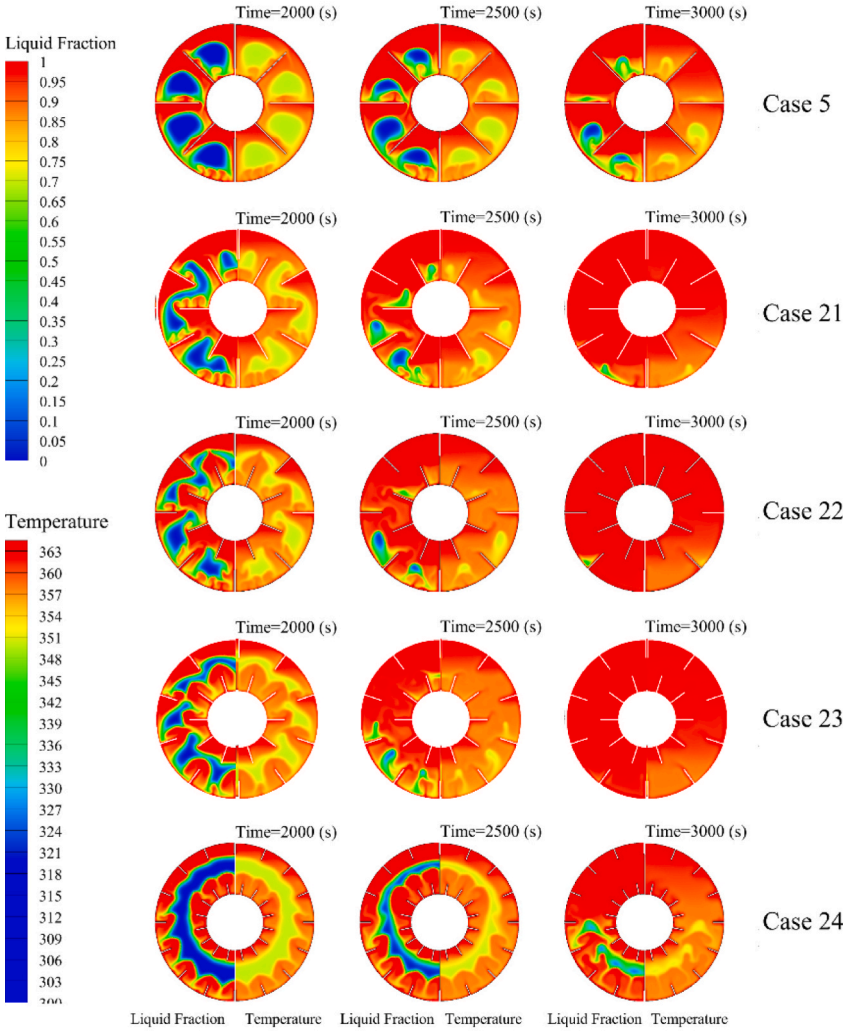

Fig. 12. (a) Liquid fraction (left half contour) and temperature (right half contour) distributions for varying fin length-number configurations. (b) Comparison of melting times for different cases.

both the number and length of fins while keeping the total PCM volume constant. The results presented in Fig. 12. show that increasing the number of fins improves heat transfer by expanding the contact area between the PCM and the fins. However, this enhancement is not purely linear, as excessive fin numbers can lead to diminishing returns. Similarly, longer fins improve conduction-based heat transfer but also reduce the volume of PCM available for thermal storage, introducing a trade-off between heat transfer efficiency and overall energy storage capacity.

The results indicate that an optimal balance exists between fin length and fin count. Configurations with moderate fin numbers and lengths tend to provide the best performance in terms of melting time reduction without significantly sacrificing energy storage capacity. The cases with 16 and 20 fins demonstrated the most effective reduction in melting time, with only minor differences between them, suggesting that beyond a certain threshold, increasing the number of fins does not significantly enhance performance. One important observation is that the positioning and attachment of fins also play a crucial role in heat transfer efficiency. In the optimized designs, the lowest fin in the TTHX was attached to the outer tube, while the remaining fins were symmetrically distributed. This symmetrical arrangement ensured uniform heat transfer and improved melting uniformity across the PCM region. From a thermal management perspective, the study highlights that while adding more fins can enhance melting performance, a limit exists beyond which additional fins provide negligible benefits. Excessively increasing the number of fins can lead to manufacturing challenges, increased material costs, and potential structural issues, particularly if the fins become too thin. The results suggest that for a fixed PCM volume, optimizing both the number and length of fins is more effective than simply maximizing either parameter independently.

4.3.4. *The effect of PCM*

The choice of phase change material (PCM) plays a critical role in determining the thermal performance of a latent heat thermal energy storage system. In the present study, two different PCMs, RT80-HC and RT82, were compared to evaluate their influence on the melting process within the triplex-tube heat exchanger (TTHX). These materials differ primarily in their latent heat of fusion and melting temperature range, both of which significantly affect heat absorption, storage capacity, and phase transition behavior. The results shown in Fig. 13 indicate that RT80-HC exhibits a higher latent heat of fusion compared to RT82, meaning it can store and release more thermal energy per unit mass. Additionally, RT80-HC has a narrower melting temperature range (77–80 °C) compared to RT82 (77–85 °C), which contributes to a more uniform and efficient phase change process. The narrower melting range allows for a more concentrated heat transfer rate, improving energy absorption efficiency and reducing thermal losses during phase transition. Despite these advantages, the simulation results show that RT80-HC leads to a slight increase in melting time compared to RT82, with a recorded difference of 1.6%. This counterintuitive result can be attributed to the fact that, while RT80-HC absorbs more energy due to its higher latent heat, the increased energy demand slightly slows down the complete melting process. However, the higher energy storage capacity

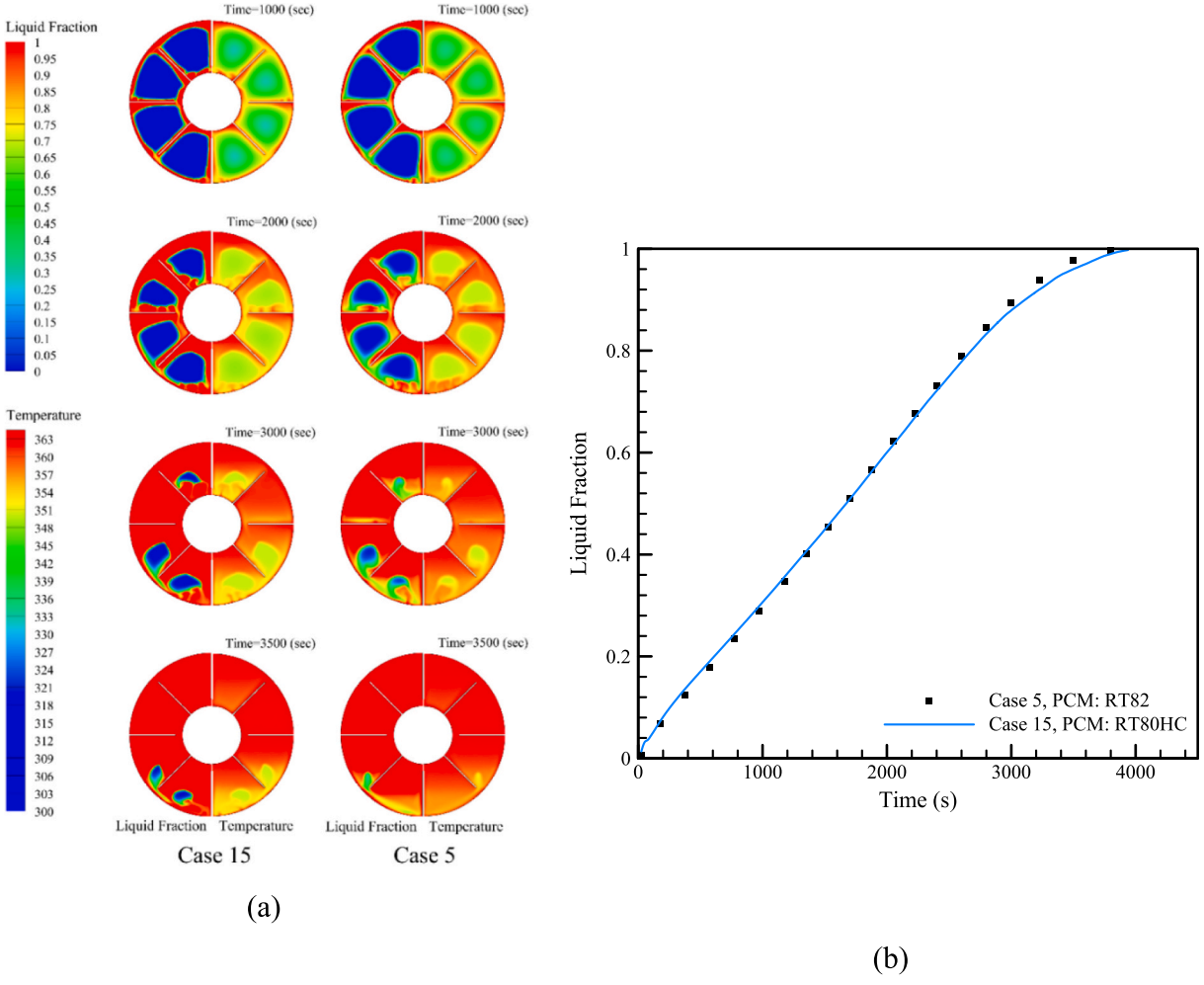

Fig. 13. (a) Liquid fraction (left) and temperature (right) distributions for RT82 and RT80-HC PCMs. (b) Liquid fraction evolution during the melting process for both PCMs.

of RT80-HC remains beneficial for applications where maximizing stored thermal energy is a priority.

The heat flux analysis further supports these findings, showing that RT80-HC achieves higher heat flux values than RT82, particularly in the early stages of melting. This behavior is linked to the proximity of the solid–liquid interface to the heat exchanger walls at the beginning of the melting process, which enhances conductive heat transfer. Over time, as natural convection becomes the dominant heat transfer mechanism, both PCMs exhibit similar melting patterns, but the higher energy absorption capacity of RT80-HC slightly extends the total melting duration. The total thermal energy stored during the charging process was found to be 1.724 MJ for RT80-HC and 1.672 MJ for RT82. While the difference in melting time is minimal, the superior energy storage capacity of RT80-HC makes it the preferable choice for applications where maximizing stored heat is essential. However, in cases where rapid charging is a priority, RT82 may offer a slight advantage due to its marginally faster melting rate.

5. Conclusions

The enhancement of charging performance in a triplex-tube thermal energy storage system by incorporating longitudinal fins and dispersing alumina (Al_2O_3) nanoparticles in phase change materials (PCMs) was numerically investigated in the present study. A two-dimensional model based on the finite-volume method was used to study the influence of fin parameters, including length, thickness, number, and orientation, as well as the effects of nanoparticle concentration and different PCM materials on the system's thermal response. The findings provide insights into optimizing latent heat thermal energy storage (LHTES) systems to improve energy efficiency and reduce charging time.

The results demonstrated that the addition of fins significantly enhances the charging process by improving heat transfer in the PCM region. Increasing the fin length and number proved to be the most effective strategy for reducing melting time, while variations in fin thickness and orientation had a comparatively minor effect. The best performance was observed in configurations with a large number of thinner fins, where the melting time was reduced by over 86% compared to the baseline case without fins. However, practical considerations such as structural integrity and manufacturing challenges must be accounted for when designing systems with ultra-thin fins.

The incorporation of nanoparticles into the PCM also contributed to faster melting by enhancing thermal conductivity. However, excessive nanoparticle concentrations (more than 4%) reduced the overall thermal storage capacity of the system, highlighting the trade-off between improved heat transfer and diminished latent heat storage. Among the PCMs studied, RT80-HC exhibited superior performance compared to RT82 due to its higher latent heat of fusion and narrower phase change temperature range.

The study also demonstrated that horizontal fin configurations slightly outperformed conventional designs by increasing the solid–liquid interface area, whereas the impact of fin orientation remained limited. Furthermore, the conjugate heat transfer effects in solid components were found to play a crucial role in accurately predicting the system's thermal behavior, emphasizing the importance of accounting for heat conduction in numerical models.

These findings provide a deeper understanding of the interplay between fin geometry, nanoparticle dispersion, and PCM selection in optimizing LHTES systems. Future research should explore advanced fin designs, such as perforated or porous structures, to further enhance melting performance while maintaining mechanical stability. Additionally, experimental validation of the proposed configurations would strengthen the reliability of numerical predictions. Investigating the long-term stability of nano-enhanced PCMs and their potential applications in large-scale thermal energy storage systems could also contribute to the development of more efficient and sustainable energy solutions.

CRediT authorship contribution statement

Ali Shahraki: Writing – review & editing, Writing – original draft, Visualization, Validation, Software, Methodology, Investigation, Formal analysis, Data curation. **Ali Tavakoli:** Writing – review & editing, Writing – original draft, Visualization, Validation, Software, Project administration, Methodology, Investigation, Formal analysis, Data curation, Conceptualization. **Majid Mohammadi:** Writing – original draft, Investigation, Formal analysis. **Amin Ebrahimi:** Writing – review & editing, Investigation. **Ali Kianifar:** Supervision.

Declaration of competing interest

The authors declare that they have no known competing financial interests or personal relationships that could have appeared to influence the work reported in this paper.

Data availability

Data will be made available on request.

References

[1] V. Baiju, Enhancing thermal performance of latent heat storage unit for solar cooling: A hybrid approach with C-shaped fins and nano-additives, Appl. Energy 351 (2023) 121825.
[2] H.M. Ali, T.-U. Rehman, M. Arıcı, Z. Said, B. Duraković, H.I. Mohammed, R. Kumar, M.K. Rathod, O. Buyukdagli, M. Teggar, Advances in thermal energy storage: Fundamentals and applications, Prog. Energy Combust. Sci. 100 (2024) 101109.
[3] N.B. Khedher, N. Biswas, H. Togun, H.I. Mohammed, J.M. Mahdi, R.K. Ibrahem, P. Talebizadehsardari, Geometry modification of a vertical shell-and-tube latent heat thermal energy storage system using a framed structure with different undulated shapes for the phase change material container during the melting process, J. Storage Mater. 72 (2023) 108365.
[4] H. Togun, H.S. Sultan, H.I. Mohammed, A.M. Sadeq, N. Biswas, H.A. Hasan, R. Z. Homod, A.H. Abdulkadhim, Z.M. Yaseen, P. Talebizadehsardari, A critical review on phase change materials (PCM) based heat exchanger: different hybrid techniques for the enhancement, J. Storage Mater. 79 (2024) 109840.
[5] R.I. Rubel, M.W. Akram, M.M. Alam, A. Nusrat, R. Ahammad, M.A. Al Bari, Phase change materials in high heat storage application: a review, Arab. J. Sci. Eng. 49 (11) (2024) 14533–14551.
[6] A. Sharma, V.V. Tyagi, C.R. Chen, D. Buddhi, Review on thermal energy storage with phase change materials and applications, Renew. Sustain. Energy Rev. 13 (2) (2009) 318–345.
[7] C.V. Podara, I.A. Kartsonakis, C.A. Charitidis, Towards phase change materials for thermal energy storage: classification, improvements and applications in the building sector, Appl. Sci. 11 (4) (2021) 1490.
[8] H. Nazir, M. Batool, F.J.B. Osorio, M. Isaza-Ruiz, X. Xu, K. Vignarooban, P. Phelan, A.M. Kannan, Recent developments in phase change materials for energy storage applications: A review, Int. J. Heat Mass Transf. 129 (2019) 491–523.
[9] S. Mat, A.A. Al-Abidi, K. Sopian, M.Y. Sulaiman, A.T. Mohammad, Enhance heat transfer for PCM melting in triplex tube with internal–external fins, Energ. Conver. Manage. (2013).
[10] Han, Y., Yang, Y., Mallick, T., Wen, C., 2022, Nanoparticles to enhance melting performance of phase change materials for thermal energy storage, nanomaterials.
[11] A.A. Al-Abidi, S. Mat, K. Sopian, M. Sulaiman, A.T. Mohammad, Internal and external fin heat transfer enhancement technique for latent heat thermal energy storage in triplex tube heat exchangers, Appl. Therm. Eng. 53 (1) (2013) 147–156.
[12] A. Tavakoli, M. Farzaneh-Gord, A. Ebrahimi-Moghadam, Using internal sinusoidal fins and phase change material for performance enhancement of thermal energy storage systems: Heat transfer and entropy generation analyses, Renew. Energy 205 (2023) 222–237.
[13] M.U. Sajid, H.M. Ali, Recent advances in application of nanofluids in heat transfer devices: A critical review, Renew. Sustain. Energy Rev. (2019).
[14] Sujith, S. V., Kim, H., and Lee, J., 2022, A review on thermophysical property assessment of metal oxide-based nanofluids: industrial perspectives, metals.
[15] A.M. Abdulateef, S.M. Jasim Abdulateef, K. Sopian, A.A. Al-Abidi, Geometric and design parameters of fins employed for enhancing thermal energy storage systems: a review, Renew. Sustain. Energy Rev. (2017).
[16] L. Kalapala, J.K. Devanuri, Influence of operational and design parameters on the performance of a PCM based heat exchanger for thermal energy storage – A review, J. Storage Mater. (2018).
[17] M. Boujelbene, H.I. Mohammed, H.S. Majdi, R. Babaei-Mahani, P. Talebizadehsardari, A. Rahbari, Melting performance of nano-enhanced phase change materials in a triple-tube heat exchanger with zigzag-shaped tubes, J. Storage Mater. 67 (2023) 107484.

[18] Z. Esmaeili, S.M. Vahidhosseini, S. Rashidi, Enhancing latent heat thermal energy storage in triplex tube heat exchangers using tree-shaped fin structures with novel branching methods, J. Storage Mater. 97 (2024) 112970.
[19] S. Gaur, R. Sahoo, J. Sarkar, Numerical investigation on thermohydraulic and exergy performance enhancement for triplex concentric tube heat exchanger using MXene nanofluids, Int. J. Energy Water Resour. (2024) 1–16.
[20] B. Hussain, M. Irfan, M.M. Khan, S. Ullah, F. ul Hasnain, Geometric optimization of fin structures for accelerated melting of phase change material in a triplex tube heat exchanger, J. Storage Mater. 79 (2024) 110162.
[21] J. Khan, K. Nithyanandam, P. Singh, Computational study on transient thermal performance enhancement of phase change materials in triplex tube heat exchanger through novel annular-finned configurations," Numerical Heat Transfer, Part A: Applications, 2024, pp. 1-18.
[22] Y.K. Liu, Y.B. Tao, Experimental and numerical investigation of longitudinal and annular finned latent heat thermal energy storage unit, Sol. Energy Mater. Sol. Cells (2022).
[23] A.A. Al-Abidi, S. Mat, K. Sopian, M. Sulaiman, A.T. Mohammad, Experimental study of PCM melting in triplex tube thermal energy storage for liquid desiccant air conditioning system, Energ. Buildings 60 (2013) 270–279.
[24] A.A. Al-Abidi, S. Mat, K. Sopian, M.Y. Sulaiman, A.T. Mohammad, Internal and external fin heat transfer enhancement technique for latent heat thermal energy storage in triplex tube heat exchangers, Appl. Therm. Eng. (2013).
[25] I. Sarani, S. Payan, A. Payan, S.A. Nada, Enhancement of energy storage capability in RT82 phase change material using strips fins and metal-oxide based nanoparticles, J. Storage Mater. (2020).
[26] RT80-HC Data sheet. rubitherm Technologies GmbH.
[27] A. D. Brent, V. R. V., K. J. Reid, 1988, Enthalpy-porosity technique for modeling convection-diffusion phase change: application to the melting of a pure metal, Num. Heat Transfer: Int. J. Comput. Methodol.
[28] A.M. Abdulateef, S. Mat, J. Abdulateef, K. Sopian, A.A. Al-Abidi, Thermal performance enhancement of triplex tube latent thermal storage using fins-nano-phase change material technique, Heat Transfer Eng. (2017).
[29] Mahdi, J. M., Nsofor, E. C., 2017, Melting enhancement in triplex-tube latent thermal energy storage system using nanoparticles-fins combination.
[30] J.M. Mahdi, S. Lohrasbi, D.D. Ganji, E.C. Nsofor, Accelerated melting of PCM in energy storage systems via novel configuration of fins in the triplex-tube heat exchanger, Int. J. Heat Mass Transf. (2018).
[31] M.M. Joybari, F. Haghighat, S. Seddeghb, A.A. Al-Abidi, Heat transfer enhancement of phase change materials by fins under simultaneous charging and discharging, Energ. Conver. Manage. (2017).
[32] F. Liu, G. Zhang, Study on melting and solidification performances improvement of phase change material using novel branch fin structure, J. Storage Mater. (2023).
[33] Palmer, B., Arshad, A., Yang, Y., We, C., 2023, Energy storage performance improvement of phase change materials-based triplex-tube heat exchanger (TTHX) using liquid–solid interface-informed fin configurations.
[34] X. Yang, X. Wang, Z. Liu, X. Luo, J. Yan, Effect of fin number on the melting phase change in a horizontal finned shell-and-tube thermal energy storage unit, Sol. Energy Mater. Sol. Cells (2022).
[35] A. Ebrahimi, C.R. Kleijn, I.M. Richardson, Sensitivity of numerical predictions to the permeability coefficient in simulations of melting and solidification using the enthalpy-porosity method, Energies 12 (22) (2019) 4360.
[36] R.S. Vajjha, D.K. Das, P.K. Namburu, Numerical study of fluid dynamic and heat transfer performance of Al2O3 and CuO nanofluids in the flat tubes of a radiator, Int. J Heat Fluid Flow (2010).
[37] M. Najafian, A. Tavakoli, A.W. Al-Fatlawi, M. Yousefi, M. Mohammadi, A. Shahraki, A. Kianifar, Accelerating melting time in a triplex tube heat exchanger thermal energy storage unit with micro-channels, J. Storage Mater. 77 (2024) 109967.
[38] A.A. Al-Abidi, S. Mat, K. Sopian, M.Y. Sulaiman, A.T. Mohammad, Experimental study of PCM melting in triplex tube thermal energy storage for liquid desiccant air conditioning system, Energ. Buildings (2013).
[39] A. Tavakoli, J. Hashemi, M. Najafian, A. Ebrahimi, Physics-based modelling and data-driven optimisation of a latent heat thermal energy storage system with corrugated fins, Renew. Energy 217 (2023) 119200.
[40] H. Eslamnezhad, A.B. Rahimi, Enhance heat transfer for phase-change materials in triplex tube heat exchanger with selected arrangements of fins, Appl. Therm. Eng. (2016).
[41] M.M. Hosseini, A.B. Rahimi, Improving heat transfer in a triplex tube heat exchanger containing phase-change materials by modications of length and position of fins, 2020, Sharif University of Technology.
[42] N.S.D.M. Khodadadi, Melting and convection of phase change materials in different shape containers: a review, Renew. Sustain. Energy Rev. (2018).
[43] T.L.B. Nourouddin Sharifi, M.J. Allen, A. Faghri, Melting and solidification enhancement using a combined heat pipe, foil approach, Int. J. Heat Mass Transf. (2014).